Pergamon

Journal of Structural Geology, Vol. 17, No. 5, pp. 709 to 725, 1995

0191-8141/95 $9.50+0.00

0191-8141(94)00090-5

Porphyroblast non-rotation during crustal extension in the Variscan Lys-Caillaouas Massif, Pyrenees

DOMINGO G. A. M. AERDEN

Laboratoire de Tectonique et Géophysique (c.p. 060), Université de Montpellier II, Place E. Bataillon, 34095 Montpellier Cedex 05, France

(*Received* 4 *May* 1993: *accepted in revised form* 10 *August* 1994)

Abstract—The dominant foliation (S_2) in the Variscan Lys-Caillaouas massif (Central Pyrenees, France/Spain) formed in a subvertical orientation during crustal thickening (D_2). Subsequent non-coaxial crustal extension produced a subhorizontal crenulation cleavage (S_3), whereby S_2 was folded and rotated. Andalusite, staurolite, cordierite and biotite porphyroblasts grew very early during this extension (D_3) and included S_2 as straight, curved and weakly crenulated inclusion trails. These inclusion trails exhibit a strong subvertical preferred orientation, which is independent of the local magnitude of D_3 strain, the dip angle of the external main foliation (S_2), or the aspect ratio and shape-orientation of porphyroblasts. This indicates that porphyroblasts did not rotate in the D_3 deformation field and hence, preserve the orientation of S_2 at the time it was trapped in the porphyroblast, relative to the bulk D_3 flow plane. Porphyroblasts could maintain a stable orientation in the D_3 flow due to complete accommodation of the bulk flow vorticity by heterogeneous shear strain. The lack of vorticity of local volumes of zero (shear) strain, such as porphyroblasts, was balanced by concentration of shear strain in planar zones anastomosing around them. It is likely that S_3 maintained a subhorizontal orientation throughout the D_3 crustal extension, which would imply that porphyroblasts also remained stationary relative to the earth's surface during D_3, whereas S_2 in the deforming matrix experienced shear-induced rotation. A late brittle-ductile folding event (D_4), involving differential rigid block rotations, dispersed the orientation of inclusion trails to some degree. These late rotations could be corrected for by artificial 'unfolding' of the F_4 folds.

INTRODUCTION

The rotational behaviour of rigid objects in ductilely deforming rock masses is currently a controversial issue. Although most structural geologists accept that this motion can be modelled by assuming relatively homogeneous viscous flow in the medium surrounding them (e.g. Ghosh & Ramberg 1976, Ildefonse *et al.* 1993, Passchier *et al.* 1993), some authors have pointed out problems with this approach (Bell 1981, 1985, Steinhardt 1989, Bell & Johnson 1989, Johnson 1990, Hayward 1992, Bell *et al.* 1992a,b, Guglielmo 1994). The orientation and microstructural data concerning porphyroblast inclusion trails of these workers indicates that ductile deformation in metamorphic rocks commonly involves pure shear components normal to the flow plane and, in contrast to homogeneous viscous flow, is governed by a strong partitioning of the flow into anastomosing planar zones of high shear strain enclosing ellipsoidal pods of lower and more coaxial progressive deformation (Fig. 1). Rheological anisotropy and the predominance of (discontinuous) solution—precipitation processes over continuous crystal-plastic processes in low–medium grade metamorphic environments has been suggested as the fundamental cause of such deformation behaviour (cf. Bell & Cuff 1989, den Brok 1989). The strain partitioning diagrams of Bell (1981) and Bell & Johnson (1992) envisage that the rotation of material lines in a general non-coaxial flow (vorticity number between 0 and 1) exclusively results from distortional components of deformation. Undeformable rock volumes would not rotate, their lack of vorticity being balanced by concentration of shear strain in planar zones anastomosing around them (Fig. 1).

The universal validity of Bell's (1981, 1985) model for ductile deformation of metamorphic rocks has been contested by Vissers (1992), Passchier *et al.* (1992), Wallis (1992), Visser & Mancktelow (1992) and Lister (1993), although Hanmer & Passchier (1991) and Passchier & Speck (1994) partially accepted the model under particular conditions. The objections of these authors have been discussed and answered by Bell *et al.* (1992a,c, 1993) and Forde & Bell (1993), but the controversy persists (e.g. Mancktelow & Visser 1993, Johnson 1993).

The correct choice of model in Fig. 1 is critical for the correct determination of shear sense from porphyroblasts with oblique S_e/S_i relationships, 'rolled' porphyroclasts and fold vergence. Contradictory answers may be obtained depending on which model is adopted (e.g. Bell & Johnson 1992). Moreover, if bulk flow planes are fixed to geographic directions, for example, to the horizontal during orogenic extension, or the vertical during orogenic thickening, porphyroblast non-rotation would imply that inclusion trails preserve the orientation of these foliations at the time they were overgrown, despite later rotation of this foliation in a deforming matrix. This is obviously valuable information for the tectonic reconstruction of fold belts.

This paper aims to help resolve the controversy concerning the (non)rotation of rigid objects in metamorphic rocks by analysing porphyroblast inclusion trail data from the Variscan Lys-Caillaouas massif in the Pyrenees. The main cleavage in this massif curves with

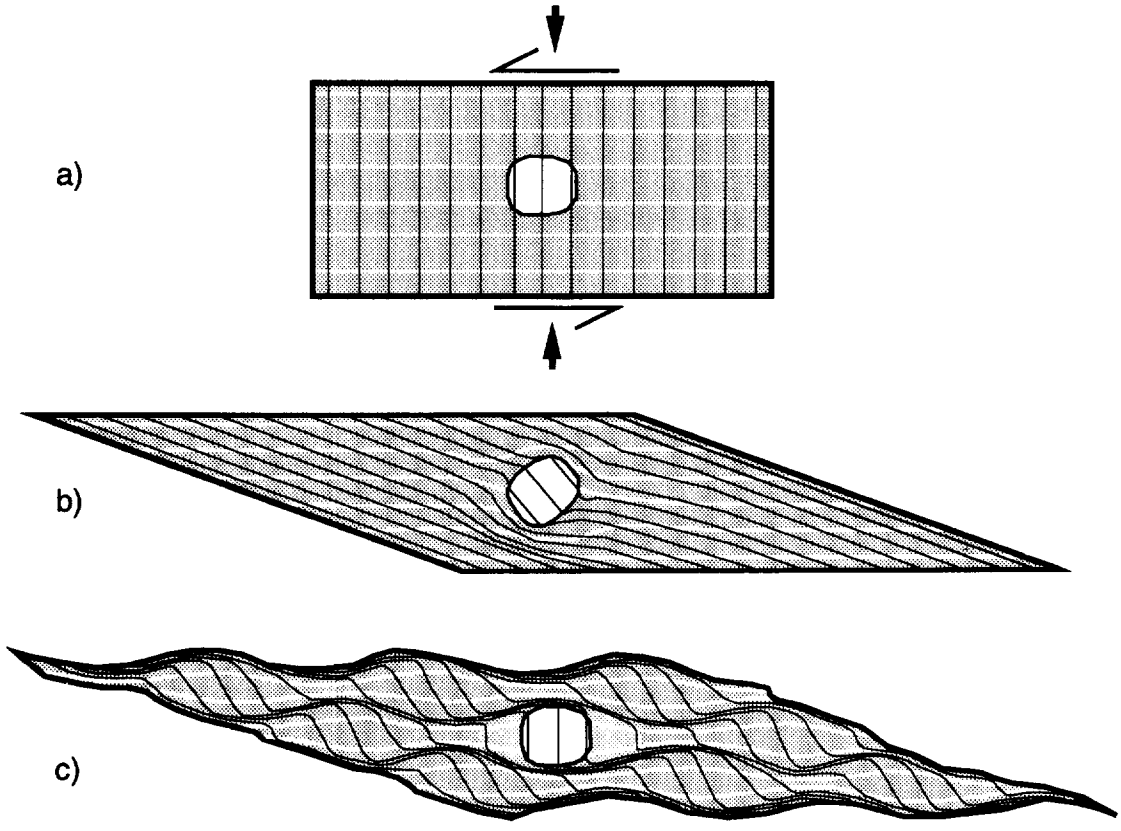

Fig. 1. Strain fields obtained by deformation of the block in (a) by a combination of pure- and simple shear. (b) Rotation model envisaging homogeneous viscous flow in the matrix and rotation of rigid objects. The object induces a local flow perturbance. (c) Non-rotation model of Bell (1981) envisaging the partitioning of strain in the flow-plane direction. The rotation of initially vertical marker lines is exclusively related to distortion components of strain. The flow remains essentially laminar around a rigid object, which does not rotate.

consistent sense into porphyroblasts, in which it continues as inclusion trails of various geometries. The angle between the external cleavage (S_{2e}) and the inclusion trails (S_{2i}) has traditionally been attributed to shear-induced southward 'rolling' of the porphyroblasts, after they overgrew the S_2 foliation (Zwart 1979, Lister *et al.* 1986, Kriegsman *et al.* 1989). This interpretation is not supported by the data collected by this author, which appears better to satisfy Bell's (1985) non-rotation model. However, this paper also describes late tectonic reorientations of groups of porphyroblasts, probably due to a later folding event that affected the Lys-Caillaouas Massif under lower metamorphic conditions. The implications of these for the use of porphyroblasts as kinematic indicators in orogenic reconstructions are discussed.

GEOLOGICAL SETTING AND DEFORMATION HISTORY

The Lys-Caillaouas Massif is part of the 'Axial Zone' of the Pyrenees, which forms the Variscan 'backbone' of the Alpine Pyrenean chain. The Massif incorporates a late-Variscan igneous complex that intruded into Cambro-Ordovician metasedimentary units consisting of amphibolite facies polydeformed biotite–andalusite–cordierite–staurolite schists and quartzites (Figs. 2 and 3a). The igneous body comprises a relatively small quartz diorite core surrounded by a much larger volume of porphyritic K-feldspar-rich granite cutting both folded bedding and the dominant foliation in the metasediments. A narrow contact metamorphic aureole is developed, characterized by (1) partial replacement of andalusite and biotite by sillimanite, (2) retrogression of staurolite, and (3) a second growth stage of andalusite, cordierite and biotite, commonly as inclusion-free overgrowth on older porphyroblast containing inclusions of S_2 (main cleavage). The intrusion thus took place after the main cleavage (S_2) development and regional peak metamorphic conditions in the Lys-Caillaouas metasediments.

Pre-Variscan deformation (D_1)

There is evidence for an early phase of large wavelength folding (D_1) pre-dating discordant deposition of the Cambro-Ordovician conglomerate unit shown in Figs. 3(a) & (b) (den Brok 1989). An S_1 cleavage associated with this unconformity has not been observed in the area.

Variscan crustal thickening (D_2)

The dominant schistosity in the Lys-Caillaouas massif (S_2) is the oldest recognized deformation microstructure

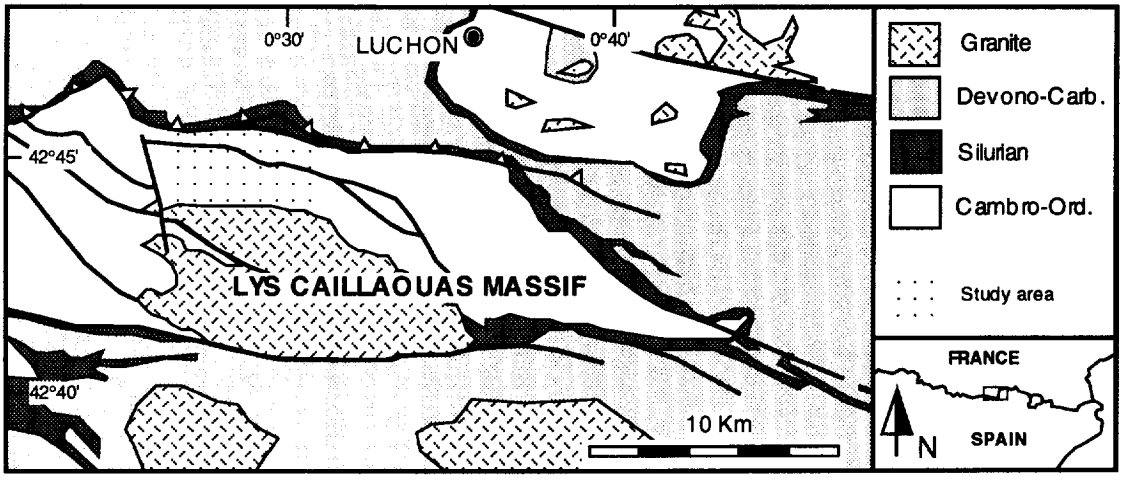

Fig. 2. Simplified map of the Lys-Caillaouas Massif in the French–Spanish Pyrenees, with the studied area (Fig. 3a) indicated.

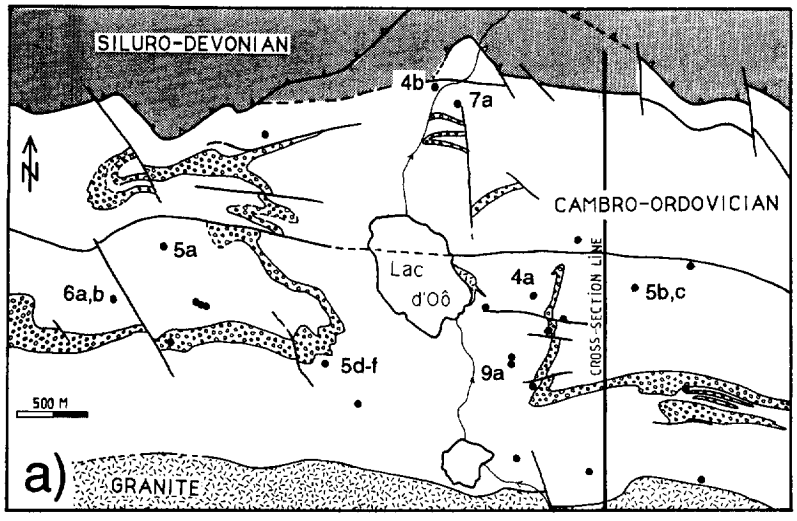

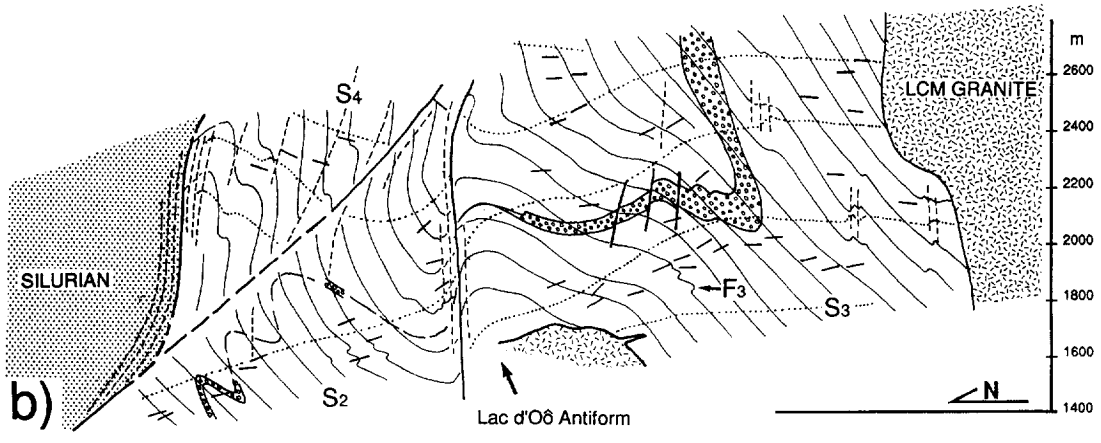

Fig. 3. (a) Simplified geological map of the study area after Aerden (1986) and Den Brok (1986). Location of map area is shown in Fig. 2. The 25 sample locations are indicated with black dots. Dot numbers correspond to figure numbers and give the respective locations of all presented microstructures. Major F_2 folds are outlined in a conglomerate unit. (b) North–south cross-section showing the attitude of S_2 (thin lines), S_3 (stippled lines) and S_4 (vertical dashed lines). Individual measurements of the orientation of S_3 are represented by small line segments. Both S_2 and S_3 are folded into an open F_4 fold known as the Lac d'Oô antiform and are cut by granite contacts. The location of the F_3 fold of Fig. 9(a) is indicated with 'F_3'.

in the area. It is mainly defined by colourless mica, trends E–W to ESE–WNW, dips gently to steeply south and is axial plane to tight F_2 folds of different scales with subhorizontal fold-axes. Zwart (1979) termed this foliation the 'main phase cleavage' as it is axial plane to the main fold generation in the Variscan Pyrenees. At suprastructural levels in the Pyrenees, S_2 is generally subvertical, whereas with structural depth and increasing metamorphic grade ('infrastructure'), S_2 progressively rotates towards the horizontal. The transition between supra- and infrastructural domains may be rather abrupt, particularly where localized within the incompetent Silurian graphitic slates. Zwart (1979) originally argued that S_2 formed in its present orientation both in supra- and infrastructure during a main phase of north–south compression and mountain building. However, later studies showed that S_2 formed in a subvertical orientation throughout the Cambro-Ordovician rock pile and became subsequently rotated to horizontal in the infrastructure only, during crustal extension (D_3; Verhoef *et al.* 1984, de Bresser *et al.* 1986, Pouget *et al.* 1988, Lister *et al.* 1986, van den Eeckhout 1986, 1990, van den Eeckhout & Zwart 1988, Corstanje *et al.* 1989, Kriegsman 1989a,b, Kriegsman *et al.* 1989, Vissers 1992, Aerden in press).

Variscan crustal thinning (D_3)

S_2 is deformed by a moderately N- and S-dipping differentiated crenulation cleavage (S_3) with E–W-trending subhorizontal crenulation axes (Fig. 3b). This crenulation cleavage is pervasively developed in the massif and is axial plane to relatively rare, cm–m scale folds that overprint larger-scale F_2 folds. Both F_3 folds and crenulations have dominantly 'Z'-asymmetries looking east and, accordingly, S_2 generally curves anticlockwise out of the quartz-rich crenulation short-limb zones ('microlithons') into the more mica-rich and narrower long-limb zones. The latter define the S_3 cleavage planes and are referred to as 'differentiation zones' (Bell 1981, Bell & Cuff 1989). The concentration (partitioning) of strain and increased quartz dissolution in these differentiation zones is well illustrated where thin quartz veinlets become boudinaged as they pass through them (Fig. 4a). Pure-shear components with principle shortening direction normal to S_3 are indicated by the symmetrical wrappings of S_3 around rigid porphyroblasts, 'millipede' microstructures (Fig. 5a) and weakly crenulated inclusion trails the axial planes of which can be traced into a matrix with tighter crenulations (Aerden in press). Sinistral simple-shear components are indicated by the dominant sense in which S_2 curves out of the microlithons into the differentiation zones, independent of the angle between S_2 in the microlithon and the microlithon wall. Rotation angles commonly exceed 90° (Figs. 6a & b), which would be inconsistent with coaxial flattening following initial buckling and flexural slip of S_2. From a microstructural point of view, the D_3 deformation is thus best interpreted as a general non-coaxial flow that rotated S_2 from an initially steep to an inclined position. This is consistent with previous kinematic interpretations of these foliations by Verhoef *et al.* (1984), van den Eeckhout (1986, 1990), de Bresser *et al.* (1986), Gibson (1991), Lister *et al.* (1986), van den Eeckhout & Zwart (1988), Pouget *et al.* (1988), Kriegsman (1989a) and Kriegsman *et al.* (1989).

Macroscopic D_3 structures can be explained as analogues to the microstructures. In the rare short-limbs of macroscopic F_3 folds, S_2 was found to dip steeply at a high angle to S_3 and to be symmetrically crenulated. In the long-limbs, S_2 dips gently at a low angle to S_3 and zones can be distinguished where S_2 is asymmetrically crenulated and where it is almost straight (not crenulated). These observations fit well with folding by progressive heterogeneous shearing, whereby S_2 progressively rotated out of an initial shortening orientation (crenulation) into an extensional orientation and was completely straightened out in the zones of maximum strain (discussed further below). At different scales of observation, the variable angle between S_2 and S_3 is thus regarded as a direct measure of strain; a high angle indicating low strain and a low angle high strain. The lack of major F_3 folds implies that deformation was relatively homogeneous at the scale of the massif. Whereas in north–south cross-section (two-dimensional) the D_3 deformation is interpreted as a heterogeneous general non-coaxial flow, D_3 extension components in an east–west (horizontal) direction indicate an oblate strain geometry in three-dimensions ($K < 1$; Aerden in press).

Granite intrusion

The Lys-Caillaouas igneous complex contains a foliation defined by the preferred orientation of biotite grains and K-feldspar megacrysts. This foliation describes dome patterns that most probably formed during granite intrusion (den Brok 1986). Field observations (den Brok 1986) and Rb–Sr whole rock analysis (Majoor 1988) indicate that the porphyritic granite was emplaced earlier than its quartz-diorite core and that both are derived from mainly crustal source rock. The granite post-dates the main folding event (D_2), regional peak metamorphic conditions (see above), as well as most of the D_3 deformation. The latter is deduced from the presence of S_3 in numerous metasediment enclaves with undeformed margins and from aplite dykes that locally intruded along S_3 cleavage planes. Kriegsman *et al.* (1989) and Kriegsman (1989b) describe a possible F_3 fold in the granite contact. A conservative constraint on the timing of granite intrusion is therefore syn- to post-D_3.

Renewed crustal thickening (D_4)

S_4 is a subvertical to steeply N-dipping spaced crenulation cleavage that is not pervasively developed in the area of study. It is well developed adjacent to subvertical E–W-trending faults with north-block-down movement components, and possible (unknown) transcurrent components (Fig. 3b). The cleavage is axial planar to kink-

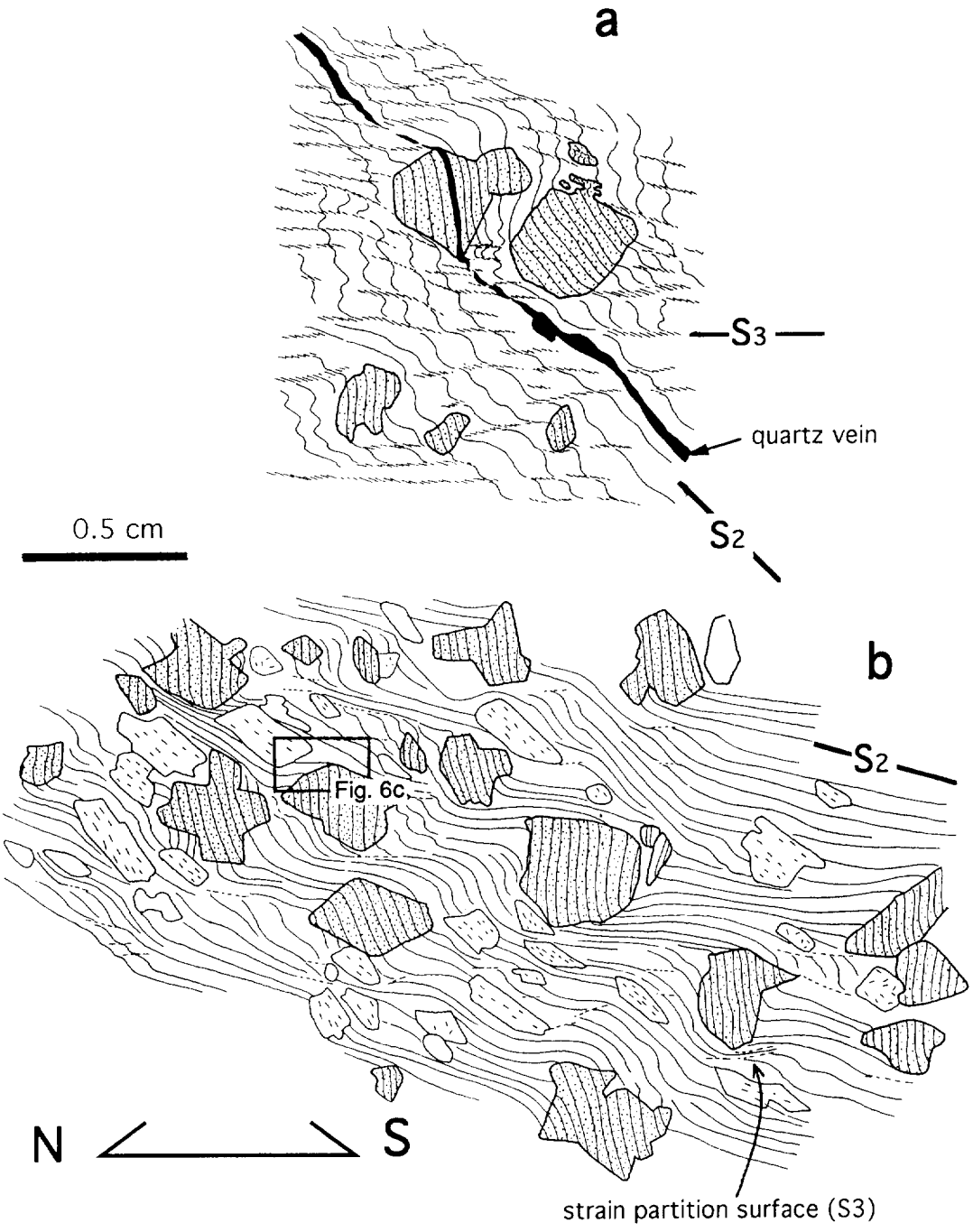

Fig. 4. (a) Line drawing of andalusite porphyroblasts, one of which is transected by a thin S_2-parallel quartz veinlet (black). The 'Z' fold outlined by the veinlet is attributed to heterogeneous D_3 shear strain. The strain-free porphyroblast preserves the initial orientation of the veinlet and S_2 relative to S_3. In the matrix, these elements have been rotated in proportion to the amount of finite shear strain. Note the concentration of sinistral shearing components in D_3 differentiation zones, witnessed by offsets and boudinage of the veinlet. Note that S_3 has the wrong shear sense for porphyroblast 'rolling'. See Fig. 3(a) for location. (b) Line drawing of staurolite (stipple) and biotite (clear) porphyroblasts with different preferred orientations, which is attributed to a different timing. Staurolite porphyroblasts preserve a subvertical S_2, subperpendicular to relics of S_3 in the matrix. Biotite porphyroblasts grew later, when S_2 had undergone considerable rotation relative to S_3. Note that the extremely constant inclusion trails in staurolite are uninfluenced by the shape or shape-orientation of porphyroblasts. The low angle between S_2 and S_3 is interpreted to indicate high shear strain in the matrix. D_3 strain partitioning surfaces are developed against porphyroblast edges. S_3 is not well developed due to extension of S_2, which may have involved destruction of earlier crenulations. See Fig. 3(a) for location.

like upright folds of variable scale with E–W-trending axes. The dominant foliation in the area (S_2) describes a large-scale F_4 fold, which is known as the 'Lac d'Oô antiform' (Zwart 1979, Fig. 3b). Minor amounts of sulphides, chlorite and other low-temperature minerals were deposited along S_4 cleavage directions and in D_4 fault zones. The faults are cut by a N-dipping Alpine thrust as the continuation of the 'Gavarnie Thrust' east of the study area (Zwart 1979). It is uncertain if the D_4 structures are also Alpine, or are late-Variscan struc-

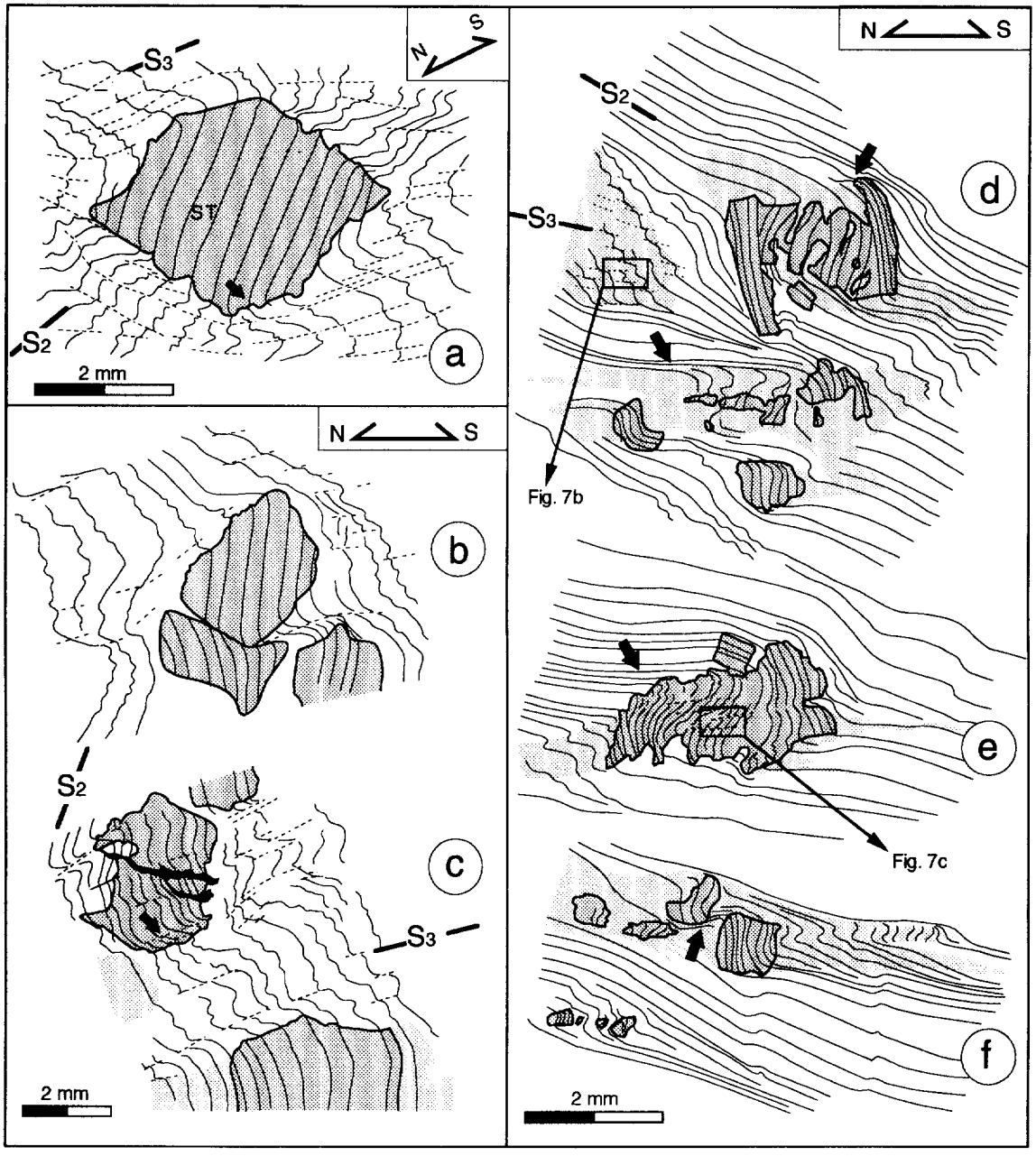

Fig. 5. (a) Millipede microstructure developed around a staurolite porphyroblast with almost straight inclusion trails. Slight curvature of the trails at the porphyroblast edge (arrow) is due to D_3 strain and indicates an early syn-D_3 timing of the porphyroblast. After porphyroblast growth, S_3 intensified and S_2 was rotated symmetrically away from the porphyroblast. See Fig. 3(a) for location. (b) & (c) Andalusite porphyroblasts from the same thin section with equally oriented straight, curved and crenulated inclusion trails. Note the relatively constant average orientation of S_2 in the matrix. Quartz-rich zones are light shaded. See Fig. 3(a) for location. (d)–(f) Andalusite porphyroblasts from a single thin section with variable inclusion trail patterns exhibiting a preferred orientation subperpendicular to traces of S_3 in the matrix. Intense shear strain in the matrix is inferred from the small angle between S_2 and S_3. Black arrows point to planar zones of D_3 strain concentration bounding zones with lower or zero strain (porphyroblasts). Porphyroblasts are inferred to have grown in F_3 micro-folds that progressively unfolded at advanced deformation stages, when S_2 entered the extensional field. The porphyroblast in (d) developed wings by uni-directional growth along the cleavage, because growth in the opposite direction was inhibited by quartz-rich strain shadows (light shaded). S_3 is preserved in a low-strain zone (Fig. 7b). The sigmoidal inclusion trails in (e) are delicately crenulated at the centre (Fig. 7c). Parallelism if these crenulations with the external S_3 in (d) demonstrates porphyroblast non-rotation during D_3. The outer (younger) porphyroblast segments do not contain crenulations, but a rotated straight S_2, consistent with a progressive decrenulation history (cf. Fig. 11). The lowermost small porphyroblasts in (f) are located in a micro-fold with an unfolding geometry. See Fig. 3(a) for location.

tures. However, they correlate well with a late fold generation associated with shear zones described elsewhere in the Pyrenees by Matte (1969; his D_3), Carreras & Cires (1986), van den Eeckhout (1986; his D_4) and Garcia-Sansegundo & Alonso (1992; their D_3 and D_4), who all favour a late-Variscan timing.

PORPHYROBLAST DATA

Inclusion trail geometry

Relative porphyroblast-matrix rotation axes in the Lys-Caillaouas Massif, as defined by the intersection of

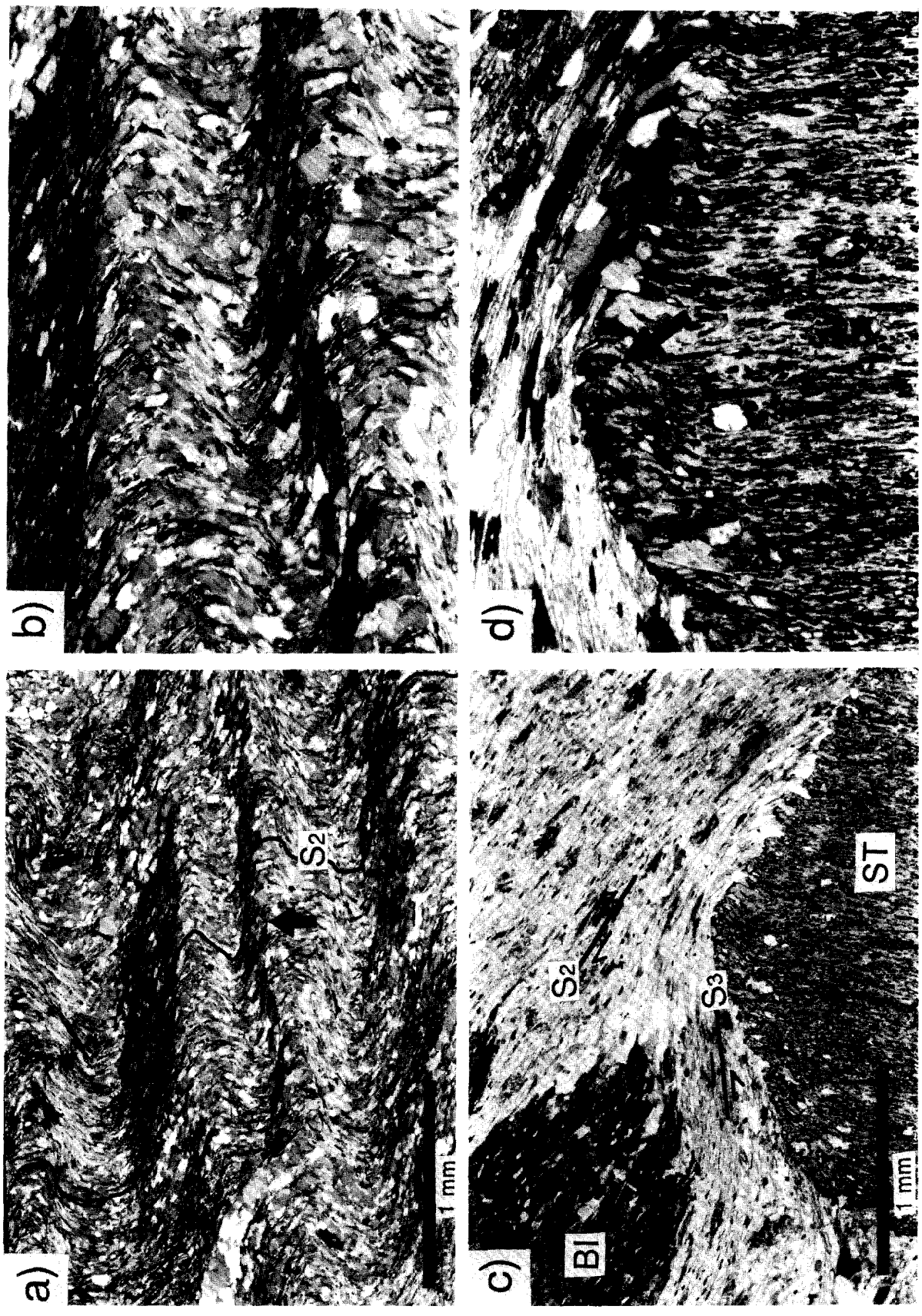

Fig. 6. (a) Photomicrograph showing the differentiated nature of the S_3 crenulation cleavage. S_3 is defined by mica-rich 'differentiation zones', in which (shear) strain was concentrated, volume was lost and where S_2 has been strongly extended and rotated. Sinistral shearing components are indicated by the sense in which S_2 rotates from low-strain, quartz-rich 'microlithons' into the differentiation zones. Rotation angles commonly exceed 90°, which is inconsistent with a coaxial deformation history, in combination with a specific starting orientation of S_2. See Fig. 3(a) for location. (b) Magnified view of the differentiation zone indicated with the arrow in 'a'. (c) Photomicrograph representing the rectangular area indicated in Fig. 4(b). The essentially straight S_2 inclusion trails of the staurolite porphyroblast are slightly deflected at the porphyroblast edge, before curving sharply into a D_3 differentiation zone in the matrix. This indicates early syn-D_3 growth in a low-strain microlithon bound by differentiation zones. Note the different orientation of inclusion trails in staurolite and biotite. (d) Magnified part of the porphyroblast in 'c'. Arrow points to the deflection in the inclusion trails.

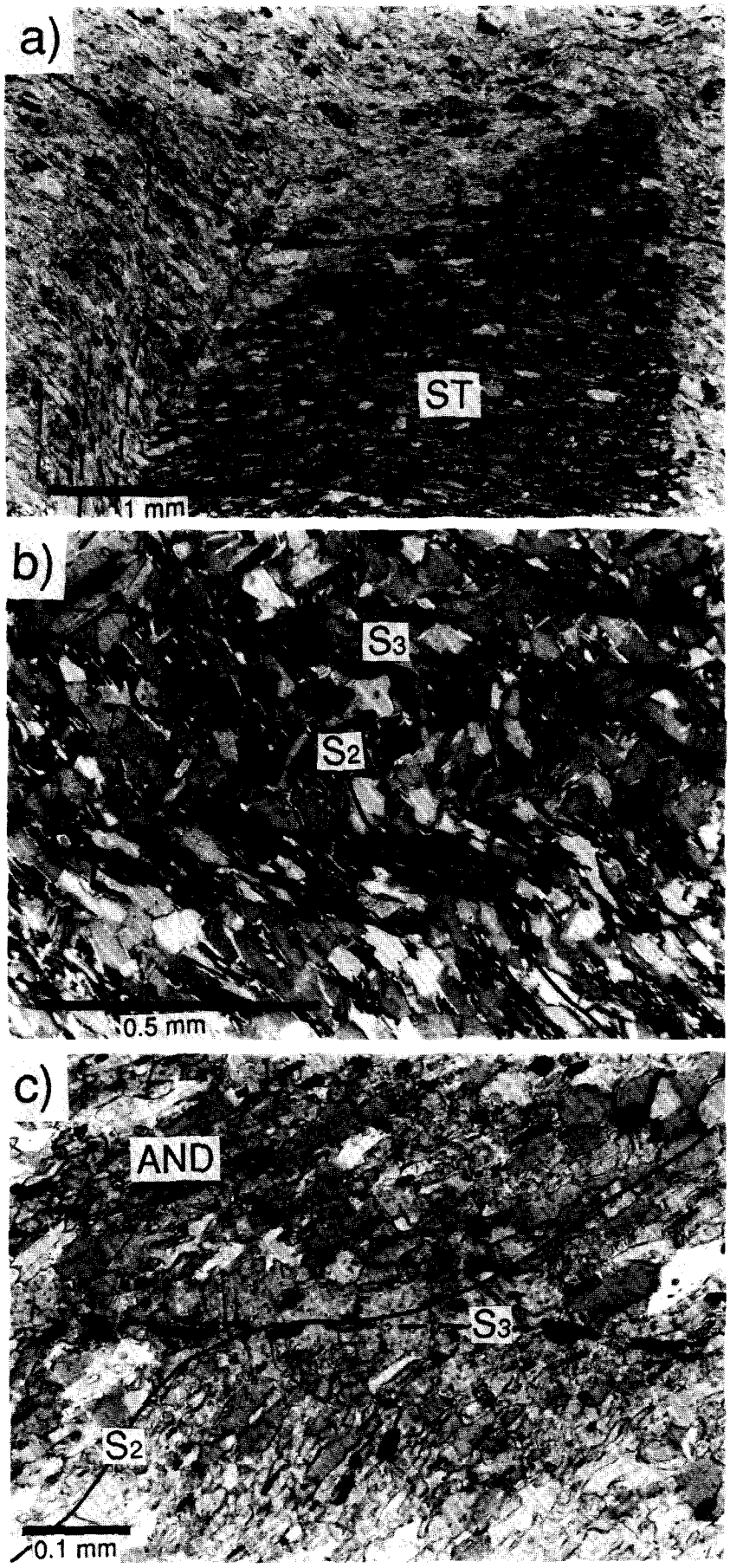

Fig. 7. (a) Photomicrograph of idiomorphic staurolite pophyroblast with straight inclusion trails (S_2). No D_2 strain-partitioning is observed, such as intensification or wrapping of S_2 around the porphyroblast's pointed edge, which suggests post-D_2 porphyroblast growth. One set of porphyroblast boundaries are parallel to S_3, suggesting that nucleation and growth was controlled by the D_3 strain partitioning pattern in the matrix (cf. Fig. 12). See Fig. 3(a) for location. (b) Relic $F_{3/2}$ crenulations preserved in the quartz-rich low-strain pod of Fig. 5(d). (c) $F_{3/2}$ crenulations preserved inside the large andalusite porphyroblast of Fig. 5(e).

the external cleavage (S_{2e}) and the inclusion trail planes (S_{2i}), trend east–west and are subhorizontal (Lister *et al.* 1986, Kriegsman *et al.* 1989, Aerden 1994). Porphyroblasts are therefore classified according to their inclusion trail geometry as observed in N–S- trending vertical thin sections. Four main types of inclusion trails geometries were distinguished: straight, curved, crenulated and 'millipede' types. However, these inclusion trail geometries are transitional with respect to each other. For example, curved inclusion trails vary between slightly sinuous and strongly sigmoidal and curved inclusion trails may be finely crenulated as well. Straight inclusion trails are by far the most common (75%), followed by curved trails (20%), crenulated (5%) and millipede types (0.3%).

Timing of porphyroblasts

Early syn-D_3 growth of porphyroblasts in the Lys-Caillaouas Massif was previously inferred by Lister *et al.* (1986), Kriegsman *et al.* (1989) and Aerden (in press). Their evidence is: (1) the continuation of S_3 from the matrix into some porphyroblasts, with the crenulations being tighter in the matrix, and (2) a switch in curvature sense of curved inclusion trails from one F_3 fold limb to the other. This evidence does not directly concern the majority of porphyroblasts that have straight inclusion trails. In principle, these could also have grown syn-D_2 and/or pre-D_3. Nevertheless, a post-D_2 to early syn-D_3 timing of these porphyroblast is also likely for three reasons.

(1) Straight inclusion trails are commonly slightly deflected at the porphyroblast rim due to D_3 strain localization against the porphyroblast edge during the very latest growth stages (Figs. 5a, 6c & d). The full gradation between straight and curved inclusion trails, the latter undisputedly syn-D_3, suggests one period of syn-D_3 porphyroblast growth. Differences in inclusion trail geometries can be attributed to local variations in the timing of D_3 strain and/or of porphyroblast nucleation.

(2) S_2 does not wrap around or intensify against the margins of porphyroblasts except, where extension and reactivation of S_2 during D_3 is indicated (discussed below). On the contrary, S_2 generally passes undeflected from the matrix into the porphyroblast, even where porphyroblasts edges project perpendicular to S_2 (Fig. 7a). The lack of D_2 deformation partitioning effects at porphyroblast edges suggest no appreciable D_2 strain after porphyroblast growth and hence, a post-D_2 timing.

(3) No appreciable differences in the spacing or quartz content between inclusion trails of different geometric types are apparent, indicating no intensification of S_2 during the period of porphyroblast growth.

Orientation of inclusion trails

The orientations of inclusion trails, as well as the axial planes of other than straight inclusion trails, were measured in vertical north–south sections for 348 porphyroblasts from 24 locations (Fig. 8a). In curved and crenulated inclusion trails, the average inclusion trail orientation was estimated. The axial planes of inclusion trails were defined by their isogons, which are relatively straight. Orientations were measured relative to the thin-section edge and then translated to 'absolute' orientations. This exercise revealed a pronounced preferred orientation of inclusion trails of 80°S (Fig. 8a) and an equally strong alignment of internal axial planes about the horizontal, subparallel to the average orientation of S_3 (Fig. 8b). All samples considered in Figs. 8(a) & (b) represent macroscopic long-limb positions. Fortunately, one porphyroblast-bearing short-limb could be sampled (location marked in Fig. 3b), the data for which is represented separately (Fig. 9a). At this location, the external S_2 cleavage dips 55°N, is moderately and symmetrically crenulated and is on average parallel to consistently straight inclusion trails, indicating no relative porphyroblast-matrix rotations.

Pre-D_4 reconstruction

The average orientation of the main cleavage (S_{2e}), the regional crenulation cleavage (S_{3e}) and the inclusion trails (S_{2i}) were plotted against each other for all samples (Fig. 9b). This showed that the angles between these structural elements are independent of variation in the orientation of S_{2e} due to the large-scale folding (Fig. 3b), hence that the D_4 deformation involved differential rigid body rotations between the samples. A pre-D_4 reconstruction of inclusion trail orientations was therefore attempted by 'unfolding' S_3, assuming a horizontal origin of this foliation. This resulted in a considerable tightening of all inclusion trail orientation maxima and their further alignment in vertical and horizontal directions (Figs. 8a & b). Note that the relatively wide scatter in the orientations of curved inclusion trails disappears almost completely in the pre-D_4 reconstruction.

In the following discussion, the observed microstructural data are considered within models envisaging rotating and non-rotating porphyroblasts during D_3 deformation, respectively. Unless specified otherwise, rotations are implicitly described as relative to the D_3 flow plane, which is assumed to have been subhorizontal and subparallel to S_3. These rotations are occasionally explicitly referred to as absolute or external rotations, in contrast to relative or internal rotations, for which a reference is specified each time.

THE ROTATION INTERPRETATION

Lister *et al.* (1986), in a study of biotite porphyroblasts from the western Lys-Caillaouas massif, showed that porphyroblasts with crenulated inclusion trails grew early syn-D_3 and had not rotated relative to S_3. This was indicated by the fact that their internal axial planes were generally subparallel to those of external F_3 crenulations. These authors proposed that such porphyroblasts grew in zones where the S_2 cleavage was oriented in the

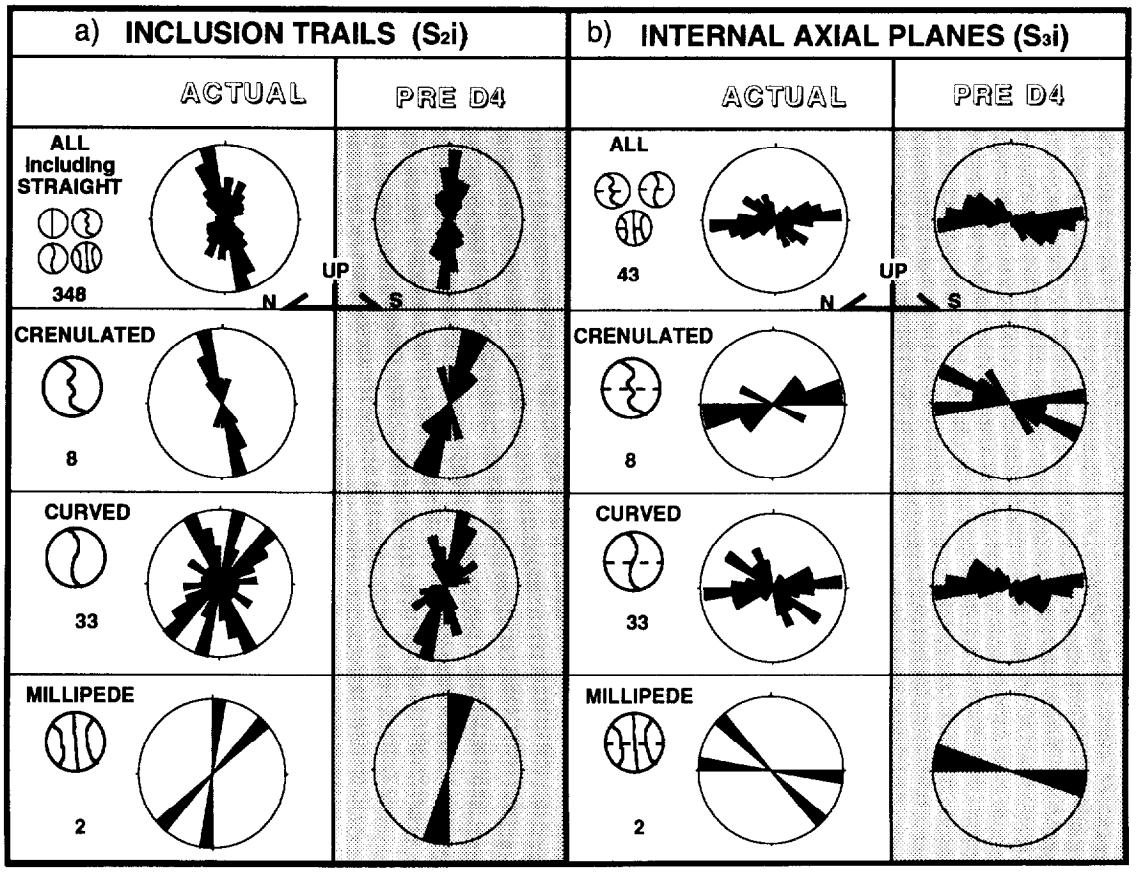

Fig. 8. Orientation plots (equal area) for inclusion trails (a) and their axial planes (b) of porphyroblasts in north–south vertical thin-sections. From top to bottom data are shown for: all porphyroblasts, porphyroblast with crenulated, curved and millipede inclusion trails. The number of measured porphyroblasts is given right of each column pair. The shaded columns give the same data after correction for the D_4 folding, by rotating S_3 in each sample to horizontal.

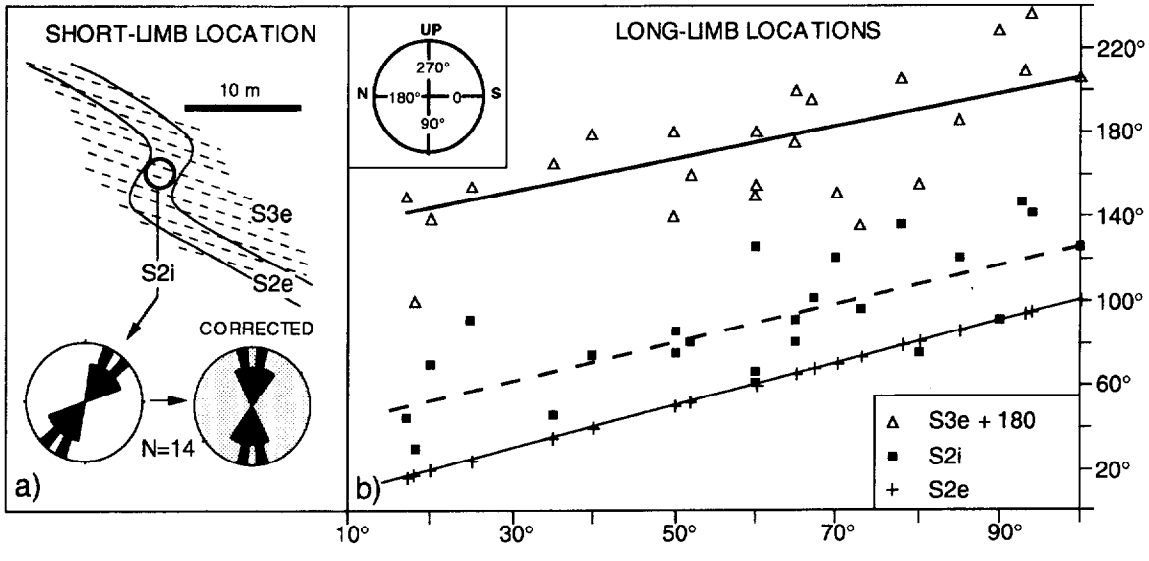

Fig. 9. (a) Orientation plots for the inclusion trails on the short-limb of a mesoscopic F_3 fold; see Figs. 3(a) & (b) for location. Inclusion trails are subparallel to (external) S_2. The pre-D_4 situation is obtained by back-rotating S_3 to horizontal, which yields subvertical inclusion trails (shaded plot) and demonstrates that inclusion trail orientations are relatively constant in F_3 folds. (b) Graph plotting the dip angle of S_2 against that of the inclusion trails and the external S_3 in all 24 locations representing F_3 long limbs. The dip angle of S_2 varies due to the presence of a large-scale F_4 fold in the area (Lac d'Oô antiform). Dashed and thick continuous lines are linear regression lines. The graph shows that the relative angles between the three microstructural elements are independent of the (external) dip angle of S_2. This suggests that the D_4 deformation produced rigid body rotations between blocks containing different samples. The average angle between S_2 and S_3 is approximately 60°.

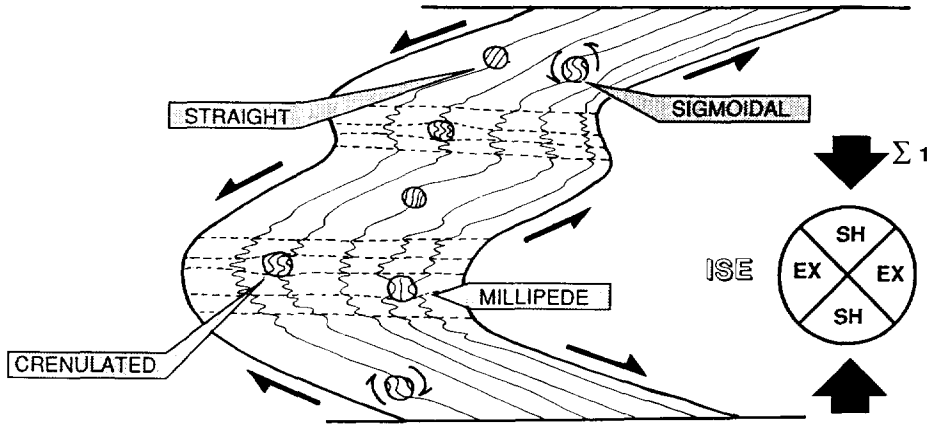

Fig. 10. Schematic illustration of the model proposed by Lister *et al.* (1983) for the synchronous development of crenulated and sigmoidal inclusion trails as a function of the orientation of S_2 in the D_3 flow field. The instantaneous strain ellipse (ISE) shows fields of incremental extension and shortening. In the fold hinges, S_2 is crenulated and porphyroblasts do not rotate. On the limbs S_2 has an extensional orientation and antithetic shearing is induced along it (solid half arrows). This would have caused porphyroblasts to rotate. Note that the rotation of porphyroblasts is to some degree balanced by opposite rotation of the fold limbs.

shortening field of the D_3 deformation (Fig. 10) and where S_2, consequently, became crenulated. On the other hand, biotite porphyroblasts with curved or sigmoidal inclusion trails would have grown in zones where the S_2 cleavage was oriented in the extensional field of the D_3 flow (e.g. on the long limbs of D_3 folds) and where the S_3 crenulation cleavage did not develop. Here, the D_3 deformation would have been accommodated by antithetic shearing along S_2, as in flexural slip folding, which would have induced rotations of porphyroblasts relative to S_2 with opposite sense on opposite fold limbs (Fig. 10).

The inclusion trail data shows no significant differences between the preferred orientation of crenulated, millipede, straight and curved inclusion trails (Figs. 8a & b). If curved and straight inclusion trails, which are oblique to the external foliation (S_2) rotated, but crenulated and millipede inclusion trails did not, the question arises why all inclusion trails are subparallel. A related question is why inclusion trail orientations are the same on opposite F_3 fold limbs, at least in the pre-D_4 reconstruction (Figs. 8a and 9a). A simple answer is that the relative porphyroblast rotations produced by shearing along S_2 (Shearing Induced Vorticity or 'SHIV' of Means *et al.* 1980) were statistically cancelled by opposite rotation of S_2 in the D_3 flow ('Spin' of Means *et al.* 1980; Fig. 10). This would explain preservation of a vertical S_2 in the form of a preferred orientation of inclusion trails. In fact, the model of Lister *et al.* (1986) would provide an alternative non-rotation model to that of Bell (1981), the difference between the models being that porphyroblast non-rotation is incidental in the former and a general principle in the latter model.

Problems with the rotation model

Although the presented porphyroblast data appear consistent with the rotation model described above, in more depth four problems are encountered.

(1) In flexural-slip folding, the fold limb rotation or 'spin' (α) is equal to the internal shearing angle ϕ, with the internal shear strain $\gamma = \tan\phi = \tan\alpha$. Experiments and fluid dynamics theory (e.g. Ghosh & Ramberg 1976, Hanmer & Passchier 1991) predict that the angular velocity of equant particles in a viscous simple-shear flow is half the shear-strain rate ($\dot{\gamma}$). Thus, the rotation angle of a rigid object, in radians, is given by $\beta^r = 1/2 \tan\alpha$. The non-linear relationship between object rotation (β) and opposite fold limb rotation (α) implies that (1) spin can generally not be cancelled by SHIV, (2) zones with different strain magnitude in the Lys-Caillaouas massif should exhibit different porphyroblast orientations, and (3) in high-strain zones with straight and low dipping S_2, the preferred orientation of inclusion trails should significantly deviate from vertical. These predictions were tested by comparing the orientation of inclusion trails in zones of contrasting deformation intensity.

For reasons outlined earlier, Figs. 4(a), 5(b) & (c) are interpreted as zones of moderate D_3 deformation where a crenulated S_2 dips steeply at a high angle with S_3. In contrast, Figs. 4(b), 5(c), (d) & (f) represent high-strain zones, in which S_2 dips at a small angle with S_3. Crenulations in the high-strain zones are only partially developed, probably due to extension of S_2 in the D_3 deformation field (discussed below). In both low- and high-strain zones inclusion trails define similar preferred orientations subperpendicular to S_3. Thus, no relationship appears to exist between finite strain magnitude and inclusion trail orientation, which is unexplained in the rotation model.

(2) The Lister *et al.* (1986) model envisages that porphyroblasts rotated, or not, depending on the orientation of S_2 in the D_3 flow and either led to sigmoidal or crenulated inclusion trails, respectively. Assuming that S_2 was straight at the onset of D_3 deformation, a relationship should thus exist between the geometry of inclusion trails and the angle between S_2 and S_3 (finite strain intensity). This was never shown. On the contrary, the present author found that pairs of porphyroblasts with sigmoidal and crenulated inclusion trails

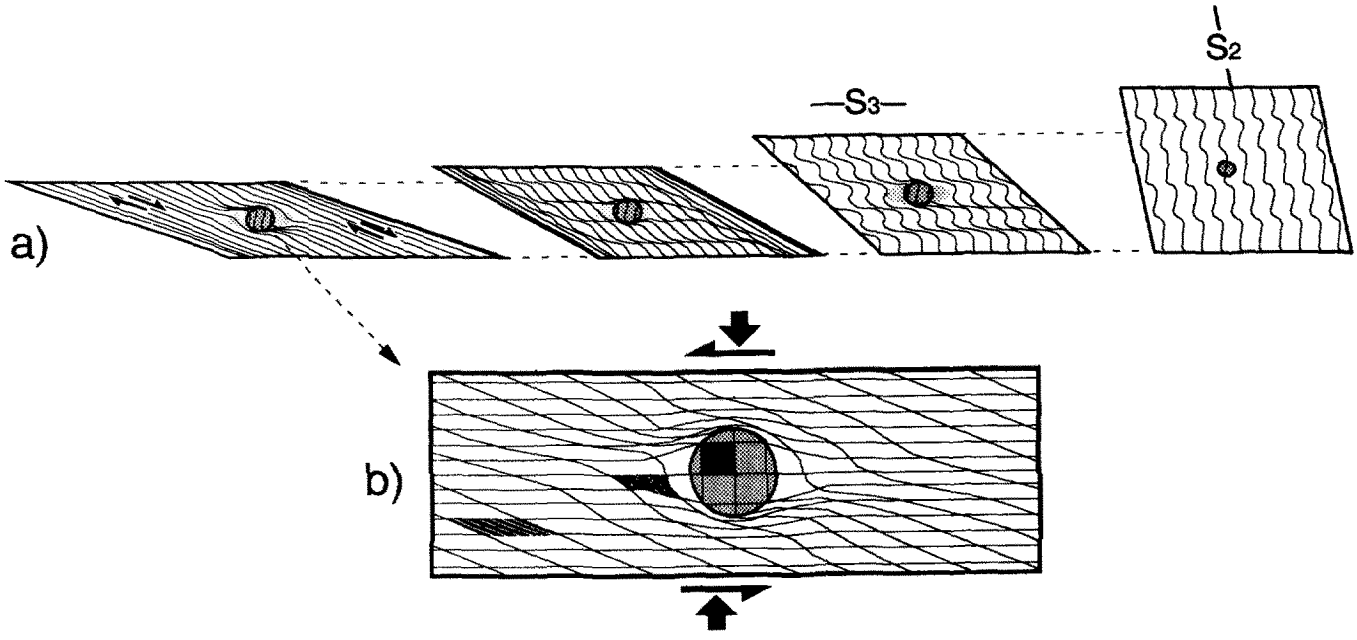

Fig. 11. (a) Line diagram showing the hypothetic deformation history of a pre-existing foliation, oriented perpendicular to the boundaries of a general non-coaxial flow. After a critical amount of strain, the foliation rotates into the extensional field of the deformation and crenulations obtain progressively more extensional geometries. Eventually, deformation becomes easier to accommodate by antithetic shearing along the anisotropy than by continued (synthetic) shearing in differentiation zones, which are gradually destroyed. (b) The anisotropy-induced shearing stage is not reached in strain-protected zones, within and adjacent to rigid objects. These zones remain separated from the matrix by differentiation zones. The latter accommodate the vorticity contrast between the object and the matrix without necessity of object rotation.

commonly occur together in a matrix with constantly oriented S_2, both in zones of low- and high-strain (Figs. 5b–f). This also aggravates problem 1 as, according to the non-rotation model, such porphyroblast pairs should have experienced equal spin due to rotation of S_2 surrounding them, but different SHIV. Yet their inclusion trails are subparallel (compare Fig. 5b with c, and 5e with d & f).

(3) Lister *et al.* (1986) and Kriegsman *et al.* (1989) proposed that porphyroblasts developed sigmoidal inclusion trails by growing synchronously with extension and shearing along S_2 during D_3. The common occurrence of porphyroblasts with sigmoidal inclusion trails, anastomosed around by a strongly developed S_3 crenulation cleavage then requires that the crenulation occurred after the shearing along S_2 and the porphyroblast rotation, for example, due to an early flexural-slip folding stage without S_3 development. However, it was shown that S_3 is present in a full range of zones characterized by different finite strains and dips of S_2. Assuming that this range represents different kinematic stages of deformation, there is no evidence for early bulk rotation of S_2 without S_3 development. Only in zones of maximum shear strain, S_{2e} may be found to be straight (no S_3) and oblique to S_{2i}. As will be discussed below, this is well explained by progressive rotation of S_2 out of a shortening—into an extensional orientation at advanced deformation stages (Fig. 11a).

(4) Experiments with rotating objects in a deforming viscous medium indicate that the amount of finite object rotation strongly depends on the shape of the object, its aspect ratio and its initial orientation in the flow (e.g. Ghosh & Ramberg 1976, Ildefonse *et al.* 1993). For example, very elongate objects tend to stabilize parallel to the flow, whereas equidimensional objects could continue to rotate indefinitely. In sharp contrast to this, inclusion trail orientations in the Lys-Caillaouas Massif can be extremely constant in groups of porphyroblasts with variable shape and aspect ratio, despite high shear strains in the matrix (e.g. Fig. 4b).

THE NON-ROTATION INTERPRETATION

An alternative model, based on the non-rotation model of Bell (1985), Bell *et al.* (1986) and Bell & Hayward (1991) will now be examined. These authors inferred that porphyroblasts generally nucleate and grow in microstructural sites of relatively coaxial strain (crenulation hinges and/or short-limb zones), which are anastomosed around by planar zones on increased shear strain (crenulation long limbs or 'differentiation zones'). Geometrical differences between inclusion trails are explained as a function of the detailed porphyroblast growth history and the local microstructural development of the matrix (Fig. 12). For instance, sigmoidal inclusion trails could form by rapid overgrowth of crenulation hinges or by prolonged growth while strain progressively intensifies against the expanding porphyroblast. Millipede microstructures and crenulated inclusion trails directly evidence the above described way of porphyroblast nucleation and growth and are not subject to dispute (Figs. 5a, c & e), in contrast to straight

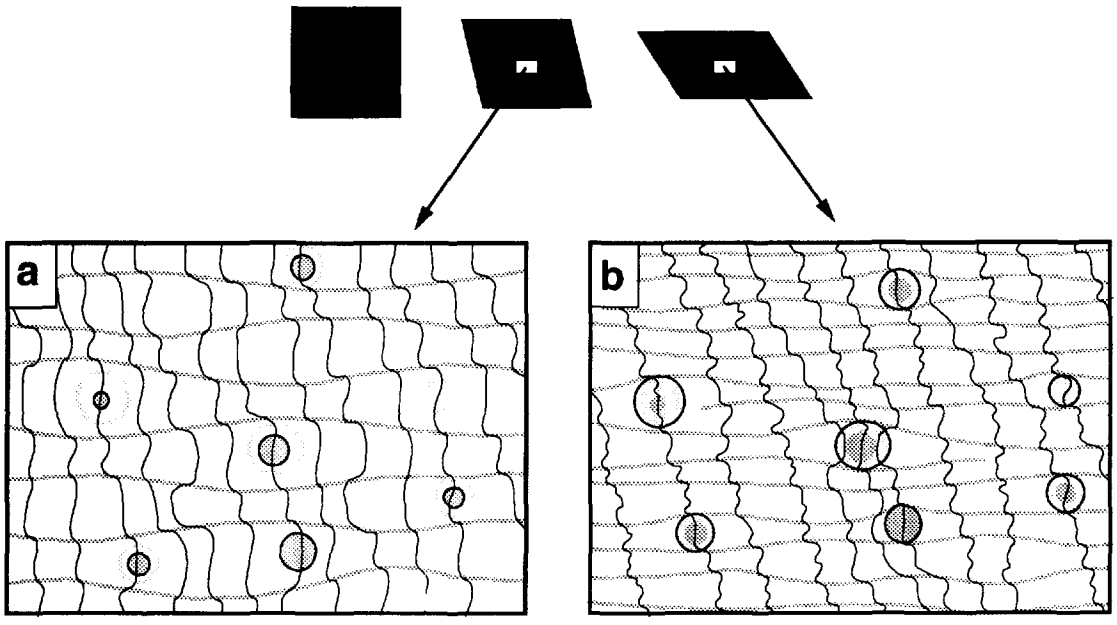

Fig. 12. Simplified non-rotation model based on the Bell *et al.* (1986) model, which explains the orientation and geometry of inclusion trails as a function of porphyroblast growth in crenulation hinges during bulk non-coaxial shortening. Two microstructural development stages are shown: (a) incipient development of a subhorizontal S_3 with porphyroblast nucleation in zones of low deformation. Faint circles mark the future porphyroblast growth stage. (b) Continued porphyroblast growth until they encounter progressively intensifying differentiation zones.

and curved inclusion trails that are oblique to the external foliation.

The preferred orientation of inclusion trails is consistent with the non-rotation model as it predicts that the orientation of S_2 at the time of porphyroblast growth (early D_3) will be preserved. Moreover, the fact that the preferred orientation is near vertical accords well with earlier interpretations of D_2 as a phase of horizontal north–south shortening and crustal thickening (e.g. Zwart 1979, Corstanje *et al.* 1989, Kriegsman *et al.* 1989, Vissers 1992). Inclusion trail curvature as a function of syn-kinematic growth in F_3 crenulations is strongly suggested by the fact that the axial planes (isogons) of inclusion trails are subparallel to S_3 (Fig. 9). This observation, together with the fact that isogons of curved inclusion trails are relatively straight represents an additional problem for rotation models, which predict curved isogons (except for rectangular porphyroblasts) in random orientations (e.g. Schoneveld 1979).

We will now return to the problems outlined earlier for the rotation model and consider them again in the context of the non-rotation model. The fact that both the orientation and the geometry of inclusion trails are independent of the magnitude of finite shear strain (problems 1, 2 and 3 for the rotation model) supports the non-rotation model as it predicts that these parameters are determined early during D_3 and are independent of the finite strain value reached (Fig. 12). Constant inclusion trail orientations despite variable porphyroblast shape (problem 4 for the rotation model) also argues in favour of the non-rotation model. The nucleation of a coherent low-strain domain on rigid objects as envisaged by this model (Fig. 1) is within certain limits independent of the object shape (Bell, 1985, 1986).

Problems with the non-rotation solution

(1) In a particular thin section two distinct preferred orientations for biotite and staurolite porphyroblasts were observed (Fig. 4b). The generally more elongate shape of the biotite crystals could be responsible for them having rotated faster than the more equidimensional staurolite crystals (Visser & Mancktelow 1992), resulting in separate orientation maxima. However, some biotite crystals are less elongate than some staurolite crystals and these exceptions still maintain the preferred orientation of their group. The different orientation maxima for biotite and staurolite are therefore more likely due to a different timing of these minerals. The smaller angle between S_{2e} and S_{2i} in biotite is consistent with a later timing, which is supported by minor biotite replacement at some staurolite edges. Additionally, staurolite inclusion trails are much more quartz-rich than the biotite trails and the matrix, which could signify progressive quartz dissolution and volume loss in the period between staurolite and biotite growth. However, in other samples inclusion trails in biotite, andalusite and staurolite porphyroblasts are all parallel, show equal quartz content and hence suggest roughly synchronous growth. The biotite porphyroblast of Fig. 4 thus appear to be anomalously late. A late biotite generation was previously recognized in the contact metamorphic aureole of the Lys-Caillaouas granite (Kriegsman *et al.* 1989) and, considering that the particular sample is derived from a low structural and erosion level in the Massif, it potentially reflects the presence of an igneous body at depth, similar to that exposed in the core of the Lac d'Oô antiform (Fig. 3b).

(2) Locally, S_3 is absent and pophyroblasts are sur-

rounded by an inclined, relatively straight S_2. Inclusion trails and internal axial planes in such porphyroblasts have the same preferred orientation as elsewhere (e.g. Figs. 4b, 5d, e & f) relative to relics of S_3 that are generally found in the same thin section. The non-rotation of these porphyroblasts (relative to S_3) is not well explained by the model of Fig. 12 showing porphyroblasts surrounded by a crenulation cleavage. To solve this difficulty the kinematic significance of the absence or presence of S_3 must be considered first.

Zones lacking a well-developed S_3, commonly preserve relics of this foliation and of F_3 microfolds in strain shadows, quartz-rich low-strain pods and inside porphyroblasts (Figs. 5d & e and 7b & c). The transitions from these domains to adjacent domains of higher strain are characterized by a decrease in the average angle between S_2 and S_3 and a progressive unfolding of crenulations and microfolds to obtain more open geometries, until they completely straighten out (Figs. 4, 5d–f; fig. 12 of Aerden in press). Such 'unfolding' or 'decrenulation' geometries are consistent with a strain path of progressive shortening (crenulation) followed by progressive extension of S_2 in the D_3 deformation field, due to rotation of S_2 out of the incremental shortening into the incremental extension field (Figs. 11a & b; Bell 1986, Aerden in press). Gradual extension of S_2 would have led to partial destruction of earlier formed F_3 crenulations, while deformation progressively changed from being partitioned into a system of differentiation zones into a pattern dominated by shearing controlled by S_2, representing the extending anisotropy (Figs. 11a & b). Such shearing or 'reactivation' of a pre-existing foliation during a subsequent deformation phase appears to be a common microstructural process in metamorphic rocks (Bell 1986, Lister *et al.* 1986, Hanmer & Passchier 1991, Aerden 1991, 1993, Hayward 1992). Some porphyroblasts with a prolonged growth history spectacularly record the rotation and progressive extension of S_2 in the D_3 flow by preserving both S_2 shortening and extension stages. At the centre of these porphyroblasts, inclusion trails are steeply oriented and locally delicately crenulated (Figs. 5e and 7c). Towards the outer and younger growth segments, inclusion trails become progressively more inclined and straighten out. The axial planes of internal crenulations and the isogons of curved inclusion trails are consistently subparallel to residual S_3 in the matrix (subhorizontal), which demonstrates synkinematic porphyroblast growth in $F_{3/2}$ microfolds and no significant porphyroblast rotation. Some peculiar 'winged' porphyroblasts (Fig. 5d) probably resulted from late-stage unidirectional growth of porphyroblasts along the S_2 fabric, because growth in the opposite direction was inhibited by quartz-rich strain shadows corresponding to earlier porphyroblast increments (Fig. 13).

Thus, porphyroblasts apparently maintained a stable orientation even after the pattern of deformation partitioning changed from S_3-parallel to S_2-parallel shearing during advanced stages of the D_3 deformation. Before this change, the deficient vorticity of porphyroblasts was compensated by concentrated shearing in differentiation zones anastomosing around them (Figs. 1 and 12). However, could this mechanism have also operated during the S_2 'reactivation' stage, when differentiation zones would have become progressively destroyed? A positive answer is suggested by the consistent presence of discrete subhorizontal strain partitioning zones at porphyroblasts edges that are subparallel to traces of S_3 elsewhere in the matrix (Figs. 4, 5d–f and 6c). Such strain partitioning zones may either consist of single differentiation zones or of somewhat broader bands in which S_2 is more gradually deflected towards an S_3-parallel orientation. The continued concentration of shear strain in these zones would have compensated the deficient distortion and vorticity of porphyroblasts as shown in Figs. 11 and 13. Residual S_3 in the strain shadows of porphyroblast and in low-strain matrix domains support the idea that S_2 and S_3 acted as antithetic and synthetic shearing systems, accommodating D_3 deformation simultaneously in zones of high- and low cumulative strain, respectively.

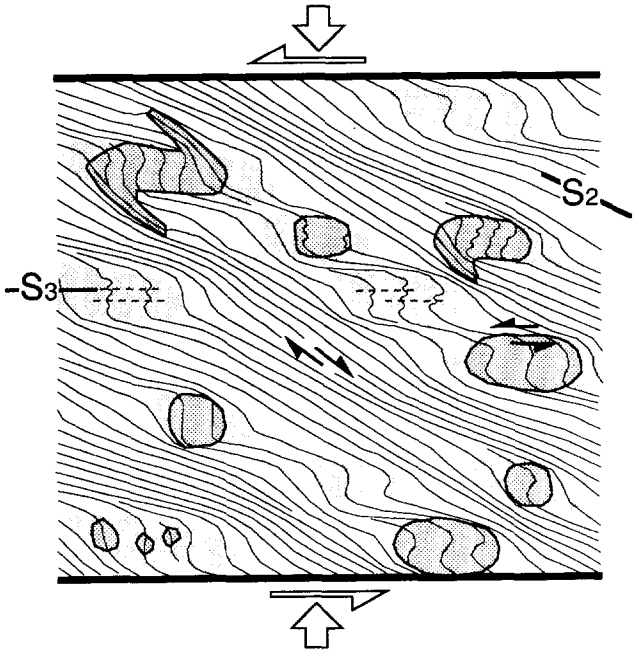

Fig. 13. Schematic representation of different porphyroblast types from the Lys-Caillaouas Massif encountered in zones where S_2 has been considerably extended during D_3 (to be compared with Figs. 4b and 5). The peculiar shape of the upper left porphyroblast resulted from uni-directional growth along S_2, due to the presence of growth-inhibiting strain shadows belonging to earlier porphyroblast segments. Porphyroblasts maintain a stable orientation even after the crenulations in which they nucleated were gradually destroyed as the result of extension of S_2. This is possible due to the continued partitioning of strain around the porphyroblasts in two shearing systems: differentiation zones with sinistral shear sense and bands of (dextral) shearing controlled by the (S_2) anisotropy being deformed. S_3 is preserved in low-strain pods.

DISCUSSION AND CONCLUSION

Role of the reference frame

It has been argued that porphyroblasts did not rotate, whereas S_2 was rotated anticlockwise in a reference

frame fixed to S_3 during D_3. However, if one chooses a reference frame that is fixed to the S_2 plane, one would describe dextral rotation of porphyroblasts. It could therefore seem that the controversy surrounding the rotation of rigid objects is merely a problem of defining a suitable reference frame. This is not the case. Fundamentally different deformation models are being considered that predict different microstructures as outlined above. One model envisages the partial partitioning of flow vorticity into rigid body rotations, whereas the other model considers its complete partitioning into distortion components of deformation.

Are porphyroblast inclusion trails a key to orogenesis?

A limited number of studies show that porphyroblasts in different metamorphic terranes may preserve vertical and/or horizontal foliations in the form of preferred orientations of overgrown foliations and/or differentiation zones, despite multiple deformations following porphyroblast growth (Steinhardt 1989, Johnson 1990, Bell & Johnson 1989, Hayward 1992, Guglielmo 1994, this study). This can be explained by assuming (1) that foliations tend to originate in vertical and horizontal orientations in large crustal volumes as the microstructural expression of bulk flow planes during crustal thickening and thinning stages, respectively, (2) that ductile deformations within an orogen are generally non-coaxial general flows, the rotational component of which are partitioned entirely as internal shear-strains (Bell 1981, 1985), and (3) that porphyroblasts commonly nucleate and grow early during deformation phases in crenulation hinge- or short-limb zones (Bell *et al.* 1986, Bell & Hayward 1991).

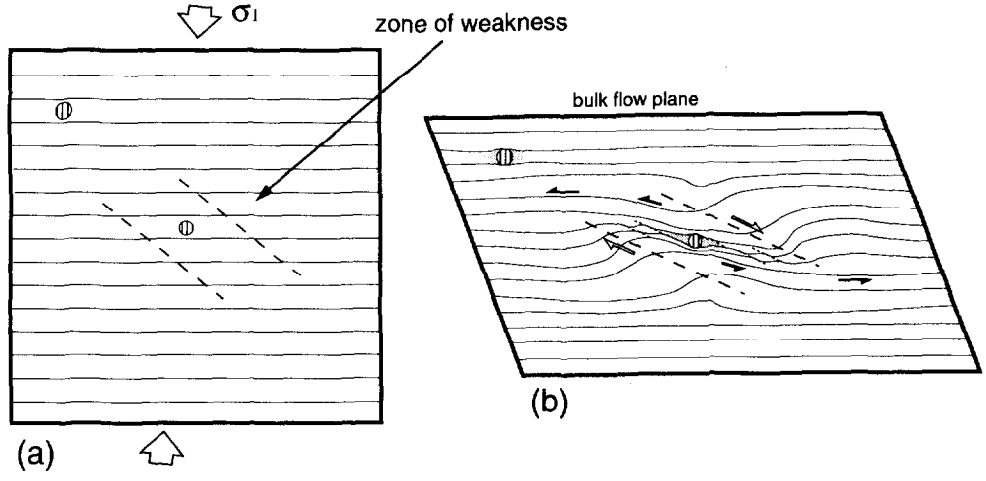

Fig. 14. Conceptual diagram showing strain partitioning around and within a planar zone of weakness (heavy stipple lines), which absorbs more strain than the surrounding material and consequently rotates relatively fast. Two complementary shearing systems, one parallel to the bulk flow plane representing the active cleavage (continuous lines) and a second, controlled by the boundaries of the zone of weakness (stippled lines), allow rigid bodies to not rotate relative to the boundaries of the flow, irrespective of their position. The rotation of an initially vertical marker line remains exclusively related to internal distortion components of deformation, even on the scale of porphyroblasts. Note that the active foliation in the zone of weakness does not remain horizontal. The secondary shear system (stippled lines) may be developed as a set of shear bands or may be more subtlely expressed as a variation in the orientation of the dominant foliation.

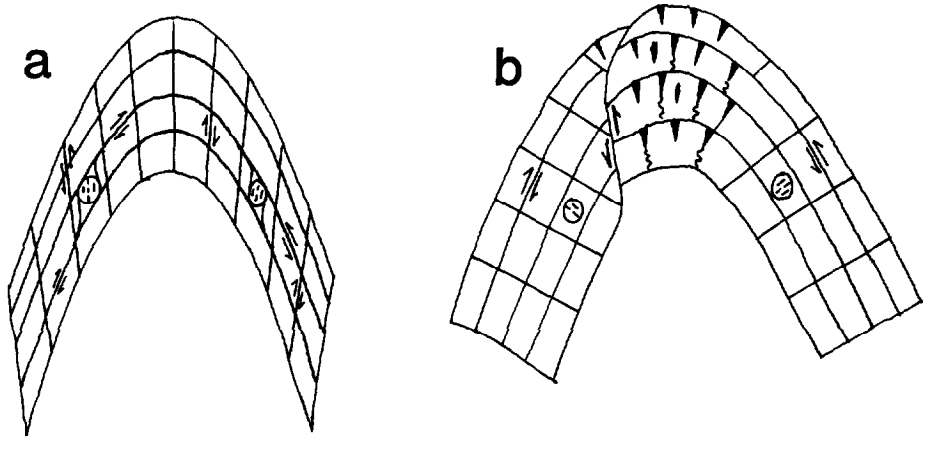

Fig. 15. Diagram illustrating the effect of ductile and brittle folding mechanisms on porphyroblast rotation. (a) Ductile folding by strain partitioning controlled by the axial plane of the fold and/or the anisotropy. The strain-incompatibility problem posed by the presence of a rigid body is solved by the partitioning of shear strain around it. Considerable bulk volume loss may accompany this deformation. (b) More brittle deformation by a combination of buckling and flexural slip folding, which cause rigid body rotations of the fold limbs. Space problems are solved by localized fracturing and dissolution in the fold hinge (black = vein; wavy lines = dissolution).

The common validity of conditions (2) and (3) has been argued and explained, but the first condition seems more difficult to assess. Bulk flow-planes in a deforming orogen can be expected to be controlled roughly by the orogen boundary conditions (approximately corresponding to that of a horizontal plate with tapered ends) and the direction of gravitational forces and externally applied forces, which could be expected to be generally vertical or horizontal. It is thus conceivable that bulk flow planes are commonly subvertical or subhorizontal in the crust during thickening and thinning stages, respectively. Foliations resulting from a laminar partitioning of such crustal-scale deformation, would form in vertical and/or horizontal orientations as well. The deformation partitioning model of Bell (1981) provides a mechanism by which porphyroblasts could maintain a stable orientation relative to the these foliations and hence, relative to bulk flow planes and the orogen boundaries. A complication is presented by lower-order boundary conditions in the crust, that is, rheological heterogeneities such as thrust ramps, basement contacts, planar anisotropy, igneous bodies, or rigid objects and planar zones of weakness. These are expected to perturb the laminar flow partitioning pattern considered so far, and to cause foliations to form in different orientations from vertical or horizontal and/or to rotate away from vertical/horizontal as they are forming. An example of such strain perturbation was discussed earlier, namely, the rotation and reactivation of S_2 as a subsidiary shearing system oblique to the bulk flow direction. It was shown that despite rotation of the internal shearing system, porphyroblasts surrounded by it remained stationary due to continued partitioning of strain around the object in S_3-parallel differentiation zones. A similar mechanism could perhaps apply more generally to crustal heterogeneities. The creation of subsidiary strain-partitioning directions, controlled by the boundaries of the spinning heterogeneity and superimposed on the main partitioning system (fixed to the bulk flow boundaries), would allow an undeformable zone/object to remain stationary even if situated within a rotating heterogeneity (Fig. 14).

I therefore do not consider it physically impossible for porphyroblasts to maintain a (sub)stable position relative to the boundaries of an orogen under a wide range of deformation conditions, in contrast to what Mancktelow & Visser (1993) suggest. In fact, the opposite seems difficult to match with the limited inclusion trail data collected so far relative to external coordinates (e.g. Bell *et al.* 1992, Hayward 1992, this study). Processes that promote porphyroblast rotation are the detachment of porphyroblasts from their matrix to form strain fringes (Miyake 1993, Aerden unpublished data) and late brittle-ductile deformation mechanisms involving a combination of kinking, flexural slip and localized dissolution and fracturing. The latter can be held responsible for the differential rigid body rotations of groups of porphyroblasts recorded in the Lys-Caillaouas Massif during D_4 (Fig. 15). The question to what extent these processes restrict the use of porphyroblasts as 'absolute' kinematic indicators for early foliations, fold axes (Hayward 1990) and stretching lineations (Aerden 1994) requires future investigations in geologically different environments.

Acknowledgements—This study was made possible by a "Human Capital and Mobility" post-doctoral fellowship from the European Commission, obtained with the support of Jacques Malavieille and Cees Passchier. I thank Simon Hanmer, Neil Mancktelow and Susan Treagus for their critical and fair assessments of earlier manuscript versions. I also thank Bas den Brok for allowing use of his thin section collection and providing continuous geological feedback. Discussions with Leo Kriegsman and Gordon Lister at Graz were as animated as they were helpful.

REFERENCES

Aerden, D. G. A. M. 1991. Foliation boudinage control on the formation of the Roseberry Pb–Zn orebody, Tasmania. *J. Struct. Geol.* **13**, 759–755.

Aerden, D. G. A. M. 1993. Formation of massive sulphide lenses by replacement of folds: the Hercules Pb–Zn Mine, Tasmania. *Econ. Geol.* **88**, 337–396.

Aerden, D. G. A. M. In press. Kinematics of orogenic collapse in the Variscan Pyrenees deduced from microstructures in porphyroblast rocks from the Lys-Caillaouas Massif. *Tectonophysics*.

Bell, T. H. 1981. Foliation development: the contribution, geometry and significance of progressive bulk inhomogeneous shortening. *Tectonophysics* **75**, 273–296.

Bell, T. H. 1985. Deformation partitioning and porphyroblast rotation in metamorphic rocks: A radical reinterpretation. *J. Metam. Geol.* **3**, 109–118.

Bell, T. H. 1986. Foliation development and refraction in metamorphic rocks, reactivation of earlier foliations and decrenulations due to shifting patterns of deformation partitioning. *J. Metam. Geol.* **4**, 421–444.

Bell, T. H. & Cuff, C. 1989. Dissolution, solution transfer, diffusion versus fluid flow and volume loss during deformation/metamorphism. *J. Metam. Geol.* **7**, 425–447.

Bell, T. H., Forde, A. & Hayward, N. 1992b. Do smoothly curved, spiral shaped inclusion trails signify porphyroblast rotation? *Geology* **20**, 59–62.

Bell, T. H., Forde, A. & Hayward, N. 1992c. Reply to comment on "Do smoothly curved, spiral shaped inclusion trails signify porphyroblast rotation?" *Geology* **20**, 1055–1056.

Bell, T. H., Forde, A. & Hayward, N. 1993. Do smoothly curved, spiral shaped inclusion trails signify porphyroblast rotation?: comment and reply. *Geology* **21**, 479–480.

Bell, T. H. & Hayward, N. 1991. Episodic metamorphic reactions during orogenesis: the control of deformation partitioning on reaction sites and reaction duration. *J. Metam. Geol.* **9**, 619–640.

Bell, T. H. & Johnson, S. E. 1989. Porphyroblast inclusion trails: the key to orogenesis. *J. Metam. Geol.* **7**, 279–310.

Bell, T. H. & Johnson, S. E. 1992. Shear sense: a new approach that resolves conflicts between criteria in metamorphic rocks. *J. Metam. Geol.* **10**, 99–124.

Bell, T. H., Johnson, S. E., Davis, B., Forde, A., Hayward, N. & Wilkins, C. 1992a. Porphyroblast inclusion-trail data; eppure non son girate. *J. Metam. Geol.* **10**, 295–308.

Bell, T. H., Rubenach, M. J. & Flemming, P. D. 1986. Porphyroblast nucleation, growth and dissolution in regional metamorphic rocks as a function of deformation during foliation development. *J. Metam. Geol.* **4**, 37–67.

Carreras, J. & Cines, J. 1986. The geological significance of the western termination of the Mérens fault at Port Vell (Central Pyrenees). *Tectonophysics* **129**, 99–114.

Corstanje, R., Klepper, C., Rutgers, B., van der Wal, I. J. & van den Eeckhout, B. 1989. Quantification of finite strain in the Pyrenean Slate Belt; a first assessment using R_f/ϕ method. *Geologie Mijnb.* **65**, 177–187.

de Bresser, J. H. P., Majoor, F. J. M. & Ploegsma, M. 1986. New insights in the structural and metamorphic history of the western Lys-Caillaouas Massif (Central Pyrenees, France). *Geologie Mijnb.* **65**, 177–187.

den Brok, S. W. J. 1989. Evidence for pre-Variscan deformation in the Lys-Caillaouas area, Central Pyrenees, France. *Geologie Mijnb.* **68**, 377–380.

den Brok, S. W. J. 1986. De geologie van het centrale Lys-Caillaouas massief ten westen en ten zuiden van Lac d'Oô. Unpublished M.Sc. thesis., Utrecht.

den Brok, S. W. J. 1992. An experimental investigation into the effect of water on the flow of quartzite. Ph.D. thesis, University of Utrecht. *Geologica Ultraiectina* **95**.

Forde, A. & Bell, T. H. 1993. The rotation of garnet porphyroblasts around a single fold in the Lukmanier Pass, Central Alps: Discussion. *J. Struct. Geol.* **15**, 1365–1368.

Garcia Sansegundo, J. & Alonso, J.-L. 1992. Stratigraphy and Structure of the southeastern Garonne Dome. *Geodinamica Acta* **3**(2), 127–134.

Gibson, R. L. 1991. Hercynian low-pressure–high-temperature regional metamorphism and sub-horizontal foliation development in the Canigou massif, Pyrenees, France—Evidence for crustal extension. *Geology* **19**, 380–383.

Ghosh, S. K. & Ramberg, H. 1976. Reorientation of inclusions by combination of pure and simple shear. *Tectonophysics* **34**, 1–70.

Guglielmo, G. Jr. 1994. Interference between pluton expansion and coaxial tectonic deformation: three-dimensional computer model and field implications. *J. Struct. Geol.* **16**, 237–252.

Hanmer, S. K. & Passchier, C. W. 1991. Shear sense indicators: a review. Geological Survey of Canada, Ottawa, paper 90-17.

Hayward, N. 1990. Determination of early fold axes orientations within multiply deformed rocks using porphyroblasts. *Tectonophysics* **179**, 353–369.

Hayward, N. 1992. Microstructural analysis of the classical spiral garnet porphyroblasts of south-east Vermont: evidence for non-rotation. *J. Metam. Geol.* **10**, 567–587.

Ildefonse, B., Sokoutis, D. & Mancktelow, N. S. 1993. Mechanical interactions between rigid particles in a deforming ductile matrix. Analogue experiments in simple shear flow. *J. Struct. Geol.* **14**, 1253–1266.

Johnson, S. E. 1990. Lack of porphyroblast rotation in the Otago Schists, South Island, New Zealand: implications for crenulation cleavage development, folding and deformation partitioning. *J. Metam. Geol.* **8**, 13–30.

Johnson, S. E. 1993. Testing models for the development of spinal-shaped inclusion tails in garnet porphyroblasts: to rotate or not to rotate, that is the question. *J. Metam. Geol.* **11**, 635–659.

Kriegsman, L. M., Aerden, D. G. A. M., Bakker, R. J., den Brok, S. W. J. & Schutjens, P. M. T. M. 1989. Variscan tectonometamorphic evolution of the Eastern Lys-Caillaouas massif, Central Pyrenees—evidence for late-orogenic extension prior to peak metamorphism. *Geologie Mijnb.* **68**, 323–333.

Kriegsman, L. M. 1989a. Deformation and metamorphism in the Trois Seigneurs massif, Pyrenees—evidence against a rift setting for its Variscan evolution. *Geologie Mijnb.* **68**, 335–344.

Kriegsman, L. M. 1989b. Structural geology of the Lys-Caillaouas massif, central Pyrenees, Evidence for large-scale recumbent folding of the late Variscan age. *Geodynamica Acta* **3**, 163–170.

Lister, G. S. 1993. Do smoothly curved, spiral shaped inclusion trails signify porphyroblast rotation?: comment and reply. *Geology* **21**, 479–480.

Lister, G. S., Boland, J. N. & Zwart, H. J. 1986. Step-wise growth of biotite porphyroblasts in pelitic schists of the western Lys-Caillaouas massif (Pyrenees).

Majoor, F. J. M. 1988. A geochronological study of the Axial Zone of the central Pyrenees, with emphasis on Variscan events and Alpine resetting, Ph.D. thesis, University of Amsterdam, Amsterdam.

Mancktelow, N. S. & Visser, P. 1993. The rotation of garnet porphyroblasts around a single fold, Lukmanier Pass, Central Alps: Reply. *J. Struct. Geol.* **15**, 1366–1372.

Matte, P. 1969. Le problème du passage de la schistosité horizontale à la schistosité verticale dans le dôme de Garonne (Paléozoic des Pyrenees Centrales). *Comptes Rendus Academie des Sciences Paris* **268**, 1841–1844.

Means, W. D., Hobbs, B. E., Lister, G. S. & Williams, P. F. 1980. Vorticity and non-coaxiality in progressive deformations. *J. Struct. Geol.* **2**, 371–378.

Miyake, A. 1993. Rotation of biotite porphyroblasts in pelitic schist from the Nukata area, central Japan. *J. Struct. Geol.* **15**, 1303–1314.

Passchier, C. W. & Speck, P. J. H. R. 1994. The kinematic interpretation of obliquely-transected porphyroblasts: an example from the Trois Seigneurs Massif, France. *J. Struct. Geol.* **16**, 971–984.

Passchier, C. W., Trouw, R. A. J., Zwart, H. J. & Vissers, R. L. M. 1992. Porphyroblast rotation: eppur si muove? *J. Metam. Geol.* **10**, 283–294.

Passchier, C. W., ten Brink, C. E., Bons, P. D. & Sokoutis, D. 1993. δ-objects as a gauge for stress sensitivity of strain rate in mylonites. *Earth Planet. Sci. Lett.* **120**, 239–254.

Pouget, P., Lamaroux, C. & Debat, F. 1988. Le dome de Bosost (Pyrénées centrales): réinterpretation majeure de sa forme et de son evolucion tectonométamorphic. *Comptes Rendus Academie des Sciences Paris* **307**(II), 949–955.

Schoneveld, C. 1979. The geometry and significance of inclusion patterns in syntectonic porphyroblasts. Ph.D. Thesis, Institute of Earth Sciences, Utrecht, The Netherlands.

Steinhardt, C. K. 1989. Lack of porphyroblast rotation in non-coaxially deformed schists from Petrel-Cove, South Australia and its implications. *Tectonophysics* **158**, 127–140.

van den Eeckhout, B. 1986. A case study of a mantled gneiss antiform, the Hospitalet massif, Pyrenees (Andorra, France). *Geologica Ultraiectina* **45**, 1–193.

van den Eeckhout, B. 1990. Evidence for large-scale recumbent folding during infrastructure formation in the Pyrenees: the structural geology of part of the eastern Hospitalet massif. *Bull. Soc. Geol. Fr.* (8), VI, **2**, 331–338.

van den Eeckhout, B. & Zwart, H. J. 1988. Hercynean crustal-scale extensional shear zone in the Pyrenees. *Geology* **16**, 135–138.

Verhoef, P. N. W., Vissers, R. L. M. & Zwart, H. J. 1984. A new interpretation of the structural and metamorphic history of the western Aston massif (central Pyrenees, France). *Geologie Mijnb.* **63**, 399–410.

Visser, P. & Mancktelow, N. S. 1992. The rotation of garnet porphyroblasts around a single fold, Lukmanier Pass, Central Alps. *J. Struct. Geol.* **14**, 1193–1202.

Vissers, R. L. M. 1992. Variscan extension in the Pyrenees. *Tectonics* **11**, 1369–1384.

Wallis, S. 1992. Comment on "Do smoothly curved, spiral shaped inclusion trails signify porphyroblast rotation?". *Geology* **20**, 1054–1055.

Zwart, H. J. 1979. The geology of the central Pyrenees. *Leid. Geol. Meded.* **33**, 191–254.